Supplementary Tables

Suppl Table 1. Primer sequences. Summary of primer sequences used in the amplification in parts or whole of *SpTERT*s and other controls.

Name	**Sequence 5'-3'**
18SF	CAGGGTTCGATTCCGTAGAG
18SR	CCTCCAGTGGATCCTCGTTA
Sally_F1	CCTCACATGAGGTTAAGAAGGAA
Sally_F2	AGGCAGTTGCCTAGCGATAC
Sally_R1	AATCGCATCCTTGGCTTG
Lucy_F2	GGGTATCAGAGATGGGCTGA
Lucy_R2	GGACTGGGCCTTGGTAGACT
SPT-X3L	TGATTCAACAGCTGAACATGG
SPT-1R	AGGGGTAGGAGCGATCATCT
SPT-EX11-10F	GCTCAACAGCATCCTAAACCA
SPT-BR	AGGAAGACATTCCTGTTGTGC

Suppl Table 2. RACE primers.

Name	**Sequence**
RLM-Outer	GCTGATGGCGATGAATGAACACTG
RLM-Inner	CGCGGATCCGAACACTGCGTTTGCTGGCTTTGATG
SPT-BL	AGACAGATCCATGGCAGGTC
SPT-BR	AGGAAGACATTCCTGTTGTGC
SPT-CL	ATCGGCCGGTCTAACTCTTG
SPT-CR	TTCTCCTCAATGACAGACTTGC
SPT-AL	TACTATTGGCGTCAGGATGG
SPT-AR	TGTCGCTCAGGTAGCATCTC
SPT-K26	TGCATCATCAACTCATCTCCA
SPT-X2L	AAGGCCTTGAAGATTGCGTA
SPT-32R	ATGGAGGGGTAGGAGCGATC

Suppl Figure Legends

Suppl. Figure 1. Genomic PCR amplification of *SpTERT*s. (A) Genomic PCR of *SpTERT-L* and *SpTERT* using exon 11 primers from five independent animals. Sperm DNA was used as a template in 1-4 and a single egg was used in 5th lane. **(B)** Estimation of the final concentration of mRNA injection in eggs by measurement of the diameter of injected sphere. **(C)** Left, measurement of telomerase activity with SE-TRAP of *S. purpuratus* eggs. linearity of the SE-TRAP assay is demonstrated by using an increasing small number of eggs (1-6 eggs). Right, the quantification of SE-TRAP products of (C) to show linearity range of assay. **(D)** Same as (C) but using 1, 2, and 4 blastula-stage embryos. Calculated densities of TRAP products were not normalized to the highest value hence setting it to one unit activity.

Suppl. Figure 2. Calculation of π and Ω. (A) A selected 30 nucleotide multiple sequence alignment is shown for six independent *SpTERT-S*. Scan windows (A-D) of 15 nucleotides define the range of which a π calculation was made and represented by a single midpoint value. Corresponding graph and table below the sequence alignment reveal the proportional values of π obtained for the level of nucleotide alignment among all 30 sites represented by four scan windows. **(B)** A selected 10 amino acid multiple sequence alignment is shown for six independent *SpTERT-S*. Each of the 10 alignment sites have explicit entropy values determined. The corresponding graph and table below the sequence alignment reveal the proportional values of Ω obtained for the level of amino acid alignment.

Suppl. Figure 3. Sample manual estimation of π. The equation shown was originally developed (Nei, 1987) as a measurement of nucleotide diversity. Denoted in the equation by π , it measures the average number of nucleotide differences per site between aligned sequence pairs. **(A)** A sample set of 6 nucleotide sequences, each of 30 nucleotides in length; an alignment was made using multiple pairwise alignment using a bootstrap of 1000 iterations by ClustalW. There appears to be 3 different specific haplotype. **(B)** The frequency of haplotype within the population, in this case 1/3 of the time for each sequence. **(C)** The pairwise population frequency (x_i*x_j) for each permutation of aligned sequence pairs. In this example, multiplying the frequency of sequence 1 multiplied by the frequency of sequence 2, yields a value of 0.11 (0.33 x 0.33), since the frequency equals 0.33 for all sequences in this population, the pairwise population frequencies all equal 0.11 accordingly. **(D)** The multiplication factor observed in front of the summation in the equation is calculated in this table, whereby n is equal to the number of sequences being analyzed. **(E)** The % nucleotide differences (π_{ij}) goes through each permutation of aligned sequence pairs per site, in this case out of a possible 30 sites (columns) in the overall alignment. In this example, between sequence 1 (SpT-S1) and sequence 4 (SpT-4) there are a total of 5 out of 30 sites that show differences in alignment between those aligned sequence pairs, therefore 5/30 = 0.17. **(F)** Multiplication of the pairwise population frequency and the % nucleotide differences for each permutation of aligned sequence pairs. **(G)** The summation of the values obtained in table F and then multiplied by the multiplication factor from table D; yielding a final value of 0.1086712, which is the average number of nucleotide differences among 30 sites between aligned sequence pairs of a total 6 sequences.

Suppl. Figure 4. Embryogenesis time course of *S. purpuratus* . Fertilized eggs were followed and photographed throughout embryogenesis. All stages including mature pluteus containing rudiment and juvenile are shown in chronological order. The pentaradial rudiment is derived from celomic sacs and gives rise to the juvenile embryo while the pluteus body undergoes cytolysis.

Suppl. Figure 5. Microinjection of *SpTERT-S* and *SpTERT-L* dominant negatives (A) Effect of SpTERT-L-DN dominant negative constructs on endogenous telomerase activity in blastula embryos. SE-TRAP analysis was carried out on 1, 2 and 4 embryos collected at blastula that were microinjected with variant forms of shown dominant negative constructs designed against *SpTERT4.0-L*. These constructs were, D996A(DN1), D1154A(DN2) and GFP mRNA and a control wild type $SpTERT_{4.0}$-*L* was used as a control. Quantification reveals that dominant negatives have no significant effect on reducing overall activity as signal intensity remains comparable to the control. **(B)** Same as (A) but using a single dominant negative (D1090A) designed against $SpTERT_{1.0}$-*S*. **(C)** Ten embryos were collected at blastula stage from each treatment (dominant negative version 1 + dominant negative version 2, *SpTERT4.0-L*, and control IVF), and subjected to RNA purification for the generation of cDNA. Quantitative RT-PCR was then carried out under the same conditions using *SpTERT-L* specific primers. *Sp18S* contained a proportion of chain terminated primers to prevent over-amplification and maintenance of linearity (see materials and methods) and is shown in each reaction lane as the internal and positive control.

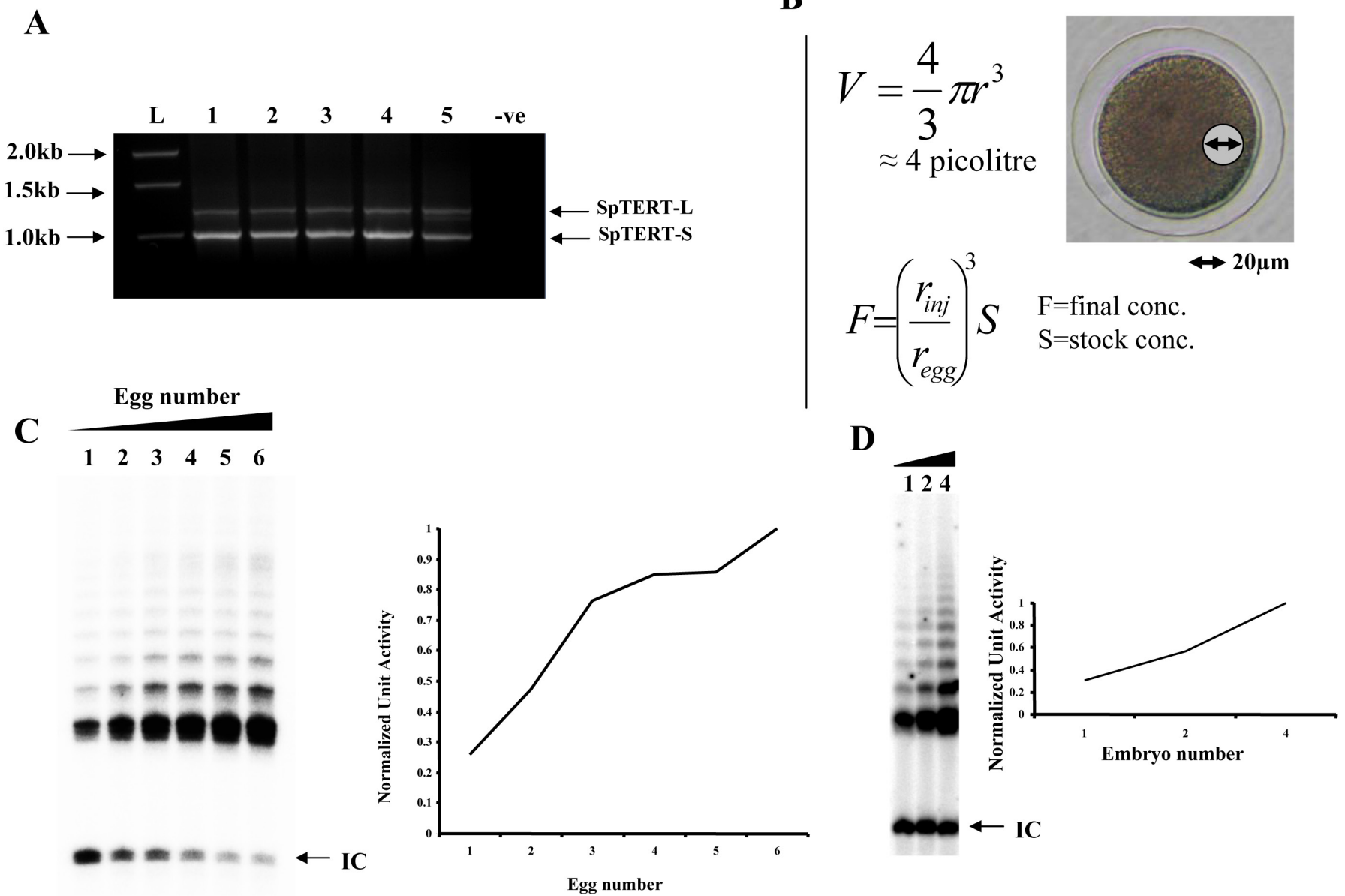

Supp Fig._1. Wells & Vaziri.

A

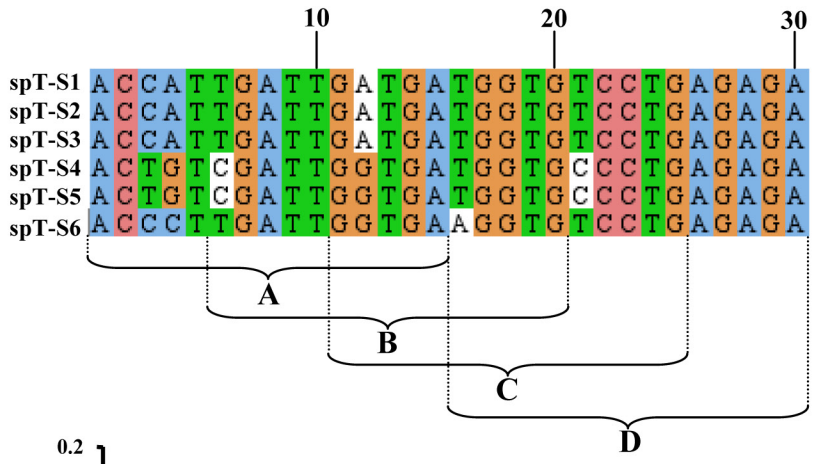

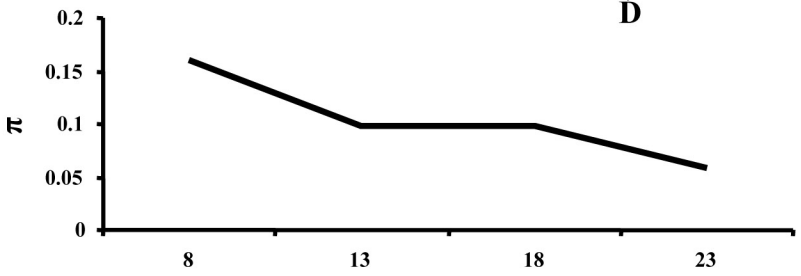

Nucleotide Scan Window	Scan Window Midpoint Position	π
A (1-15)	8	0.16000
B (6-20)	13	0.09778
C (11-25)	18	0.09778
D (16-30)	23	0.05778

B

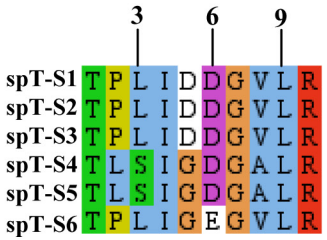

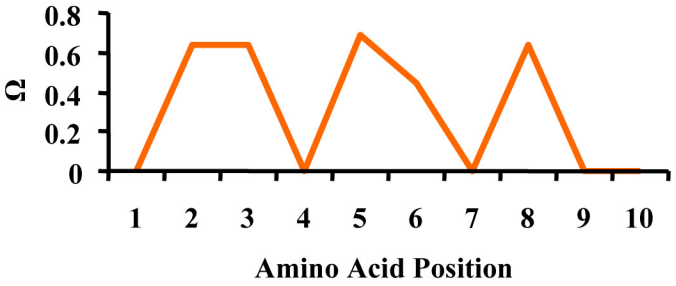

Amino Acid Position	Ω
1	0
2	0.63651
3	0.63651
4	0
5	0.69315
6	0.45056
7	0
8	0.63651
9	0
10	0

Suppl Fig._2. Wells & Vaziri.

A

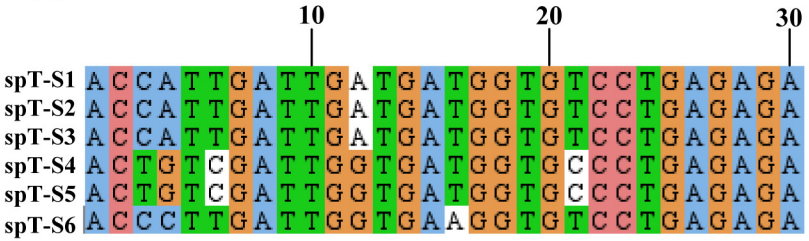

B

Sequence	Frequency
1	0.333
2	0.333
3	0.333
4	0.333
5	0.333
6	0.333

C

Pairwise Population Frequency = $x_i * x_j$						
i / j	**1**	2	3	4	5	6
1						
2	0.11					
3	0.11	0.11				
4	**0.11**	0.11	0.11			
5	0.11	0.11	0.11	0.11		
6	0.11	0.11	0.11	0.11	**0.11**	

D

n	n-1	n/(n-1)
6	5	1.2

E

% Nucleotide Differences = π_{ij}						
i / j	**1**	2	3	4	5	6
1						
2	0.00					
3	0.00	0.00				
4	**0.17**	0.17	0.17			
5	0.17	0.17	0.17	0.00		
6	0.10	0.10	0.10	0.17	**0.17**	

F

ij	$x_i x_j \pi_{ij}$
12	0
13	0
14	0.0184815
15	0.0184815
16	0.0110889
23	0
24	0.0184815
25	0.0184815
26	0.0110889
34	0.0184815
35	0.0184815
36	0.0110889
45	0
46	0.0184815
56	0.0184815

G

$\Sigma x_i x_j \pi_{ij}$	$\pi = n/(n-1) * \Sigma$ xixjπij	π/2
0.1811187	0.2173424	0.1086712

$$\hat{\pi} = \frac{2n}{n-1} \sum_{ij} \hat{x}_i \hat{x}_j \pi_{ij}$$

Suppl Fig._3. Wells & Vaziri.

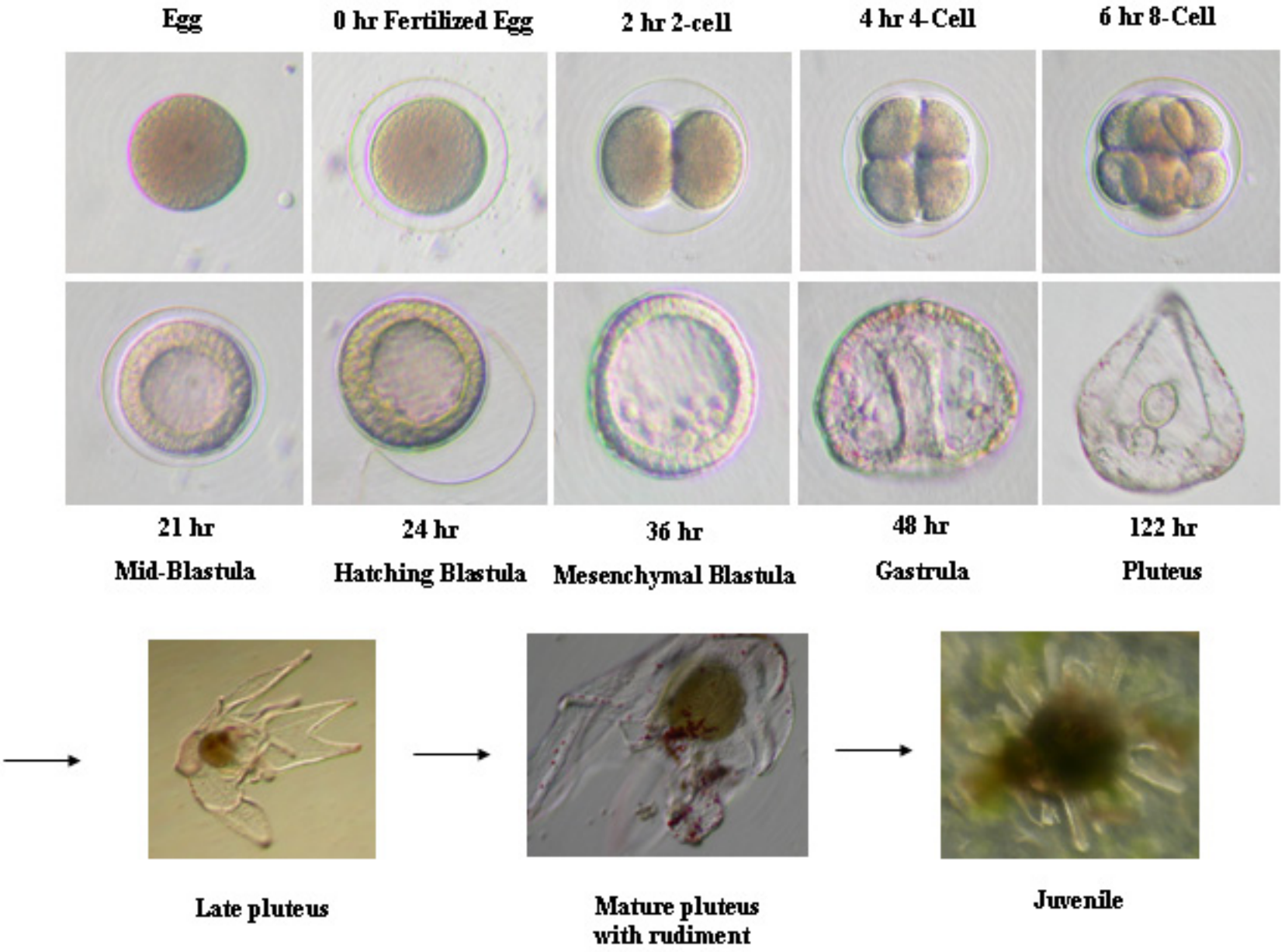

Suppl Fig._4. Wells & Vaziri.

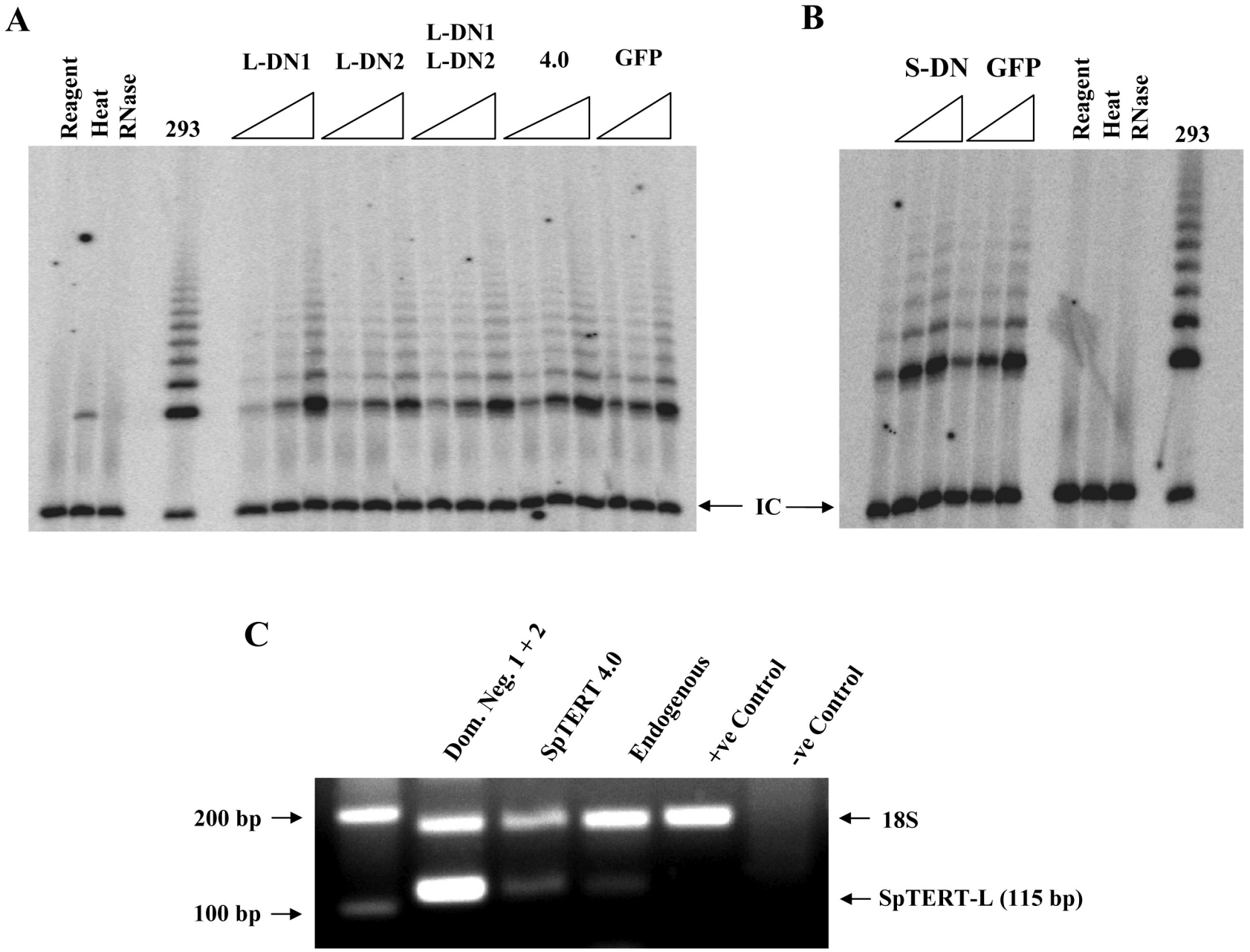

Suppl Fig._5. Wells & Vaziri.

GenBank accession numbers

The following GenBank accession numbers correspond to the *SpTERT* sequences reported and analyzed in Figures 2 and 4. The analysis of π in Figure 4 included 9 *SpTERT-S* and 10 *SpTERT-L* Exon 11 sequences.

Full Length *SpTERT* sequences: FJ615755 (*SpTERT* 1.0); FJ615756 (*SpTERT* 2.0); FJ615757 (*SpTERT* 4.0); FJ615758 (*SpTERT* 5.0); FJ615759 (*SpTERT* 6.0); FJ615760 (*SpTERT* 7.0); FJ615761 (*SpTERT* 8.0).

Exon 11 *SpTERT* sequences: accFJ615755 (SpT-Exon11-S1); accFJ615758 (SpT-Exon11-S2); FJ615762 (SpT-Exon11-S3); FJ615763 (SpT-Exon11-S4); FJ615764 (SpT-Exon11-S6); FJ615765 (SpT-Exon11-S7); FJ615766 (SpT-Exon11-S8); FJ615767 (SpT-Exon11-S11); FJ615768 (SpT-Exon11-S15); FJ615769 (SpT-Exon11-L4); FJ615770 (SpT-Exon11-L7); FJ615771 (SpT-Exon11-L8); FJ615772 (SpT-Exon11-L9); FJ615773 (SpT-Exon11-L10); accFJ615756 (SpT-Exon11-L11); accFJ615757 (SpT-Exon11-L12); accFJ615759 (SpT-Exon11-L13); accFJ615760 (SpT-Exon11-L14); accFJ615761 (SpT-Exon11-L15).